PAPER • **OPEN ACCESS**

In situ study of two-dimensional dendritic growth of hexagonal boron nitride

To cite this article: Janina Felter *et al* 2019 *2D Mater.* **6** 045005

View the article online for updates and enhancements.

This content was downloaded from IP address 134.94.122.142 on 15/08/2019 at 13:06

2D Materials

OPEN ACCESS

RECEIVED
10 January 2019

REVISED
9 May 2019

ACCEPTED FOR PUBLICATION
12 June 2019

PUBLISHED
1 July 2019

Original content from this work may be used under the terms of the Creative Commons Attribution 3.0 licence.

Any further distribution of this work must maintain attribution to the author(s) and the title of the work, journal citation and DOI.

PAPER

In situ study of two-dimensional dendritic growth of hexagonal boron nitride

Janina Felter[1,2], **Miriam Raths**[1,2], **Markus Franke**[1,2] **and Christian Kumpf**[1,2]

[1] Peter Grünberg Institut (PGI-3), Forschungszentrum Jülich, 52425 Jülich, Germany
[2] Jülich Aachen Research Alliance (JARA)—Fundamentals of Future Information Technology, 52425 Jülich, Germany

E-mail: c.kumpf@fz-juelich.de

Keywords: hexagonal boron nitride, dendritic growth, dehydrogenation limited aggregation, low energy electron microscopy (LEEM)

Supplementary material for this article is available online

Abstract

Hexagonal boron nitride, often entitled the 'white graphene' because of its large band gap, is one of the most important two-dimensional (2D) materials and frequently investigated in context with stacked arrays of single 2D layers, so called van der Waals heterostructures. Here, we concentrate on the growth of hBN on the coinage metal surface Cu(1 1 1). Using low energy electron microscopy and diffraction, we investigate the self-terminated growth of the first layer *in situ* and in real time. Most prominently, we find dendritic structures with three strongly preferred growth branches that are mostly well aligned with the Cu(1 1 1) substrate and exhibit a three-fold symmetric shape. The observation of dendritic structures is very surprising since hBN was found to grow in compact, triangular-shaped islands on many other metal substrates, in particular, on transition metal surfaces where it shows a much stronger interaction to the surface. We explain the unexpected dendritic growth by an asymmetry of the bonding energy for the two possible ways a borazine molecule can attach to an existing hBN island, namely either with one of its boron or one of its nitrogen atoms. We suggest that this asymmetry originates from different dehydrogenation states of the adsorbed borazine molecules and the hBN islands. We call this mechanism 'Dehydrogenation Limited Aggregation' since it is generic in the sense that it is merely based on different dehydrogenation energies for the involved building blocks forming the 2D layer.

1. Introduction

Hexagonal boron nitride (hBN) is a prominent and frequently studied member of the family of two-dimensional (2D) materials. It forms a hexagonal honeycomb structure of nitrogen and boron atoms, similar to graphene. Due to its structural and electronic properties, in particular its insulating nature (direct band gap of 5.97 eV [1]), it is of highest interest as part of hetero-epitaxial systems in conjunction with other 2D materials or organic thin films [2, 3]. However, the production of high quality hBN monolayers and organic thin films on hBN necessitates a deep understanding of nucleation and growth of these materials.

Single hBN layers are typically produced either by mechanical ex-foliation of single crystals [4] or *in situ* via a catalytic process on the hot metal surfaces by dissociation of borazine or other precursors [5–12]. Especially the latter has a high potential as scalable method and guarantees the lowest level of contaminations. The growth of hBN via chemical vapour deposition was studied on several metal substrates [13]. Generally, the degree of reactivity of the substrate has strong influence on the growth rate and on the morphology of the hBN layer [13–18]. For highly reactive metals, strongly corrugated and buckled films were found while with decreasing reactivity the films become more flat and weakly bonded to the substrate. This weak bonding could be very important for processes where the substrate has to be etched away for further device production and, additionally, could lead to the decoupling of molecular adsorbates on hBN from the metal states [19].

The Cu(1 1 1) surface has been recently shown to exhibit a rather weak hBN-metal interaction. Using scanning tunneling microscopy (STM), Joshi *et al* [20] found a Moiré-like superstructure caused by the lattice

© 2019 IOP Publishing Ltd

mismatch between the substrate and the hBN layer. Whether or not this finding originates from a geometric modulation (vertical buckling of lateral distortion) or from merely electronic effects is still under debate. The authors of [20] themselves conclude that the Moiré is caused by electronic contrast, since the pattern is seen only at certain, relatively high bias voltages. This is supported by x-ray standing waves (XSW) results of Brülke *et al* [15], who report relatively large bonding heights for nitrogen and boron (3.25(2) Å and 3.22(3) Å, respectively), no significant vertical buckling of the hBN layer and no indications of lateral distortions. Additionally, using high resolution spot profile analysis low energy electron diffraction (SPA-LEED), these authors found various azimuthal orientations of hBN domains with respect to the substrate, which is also an indication for a relatively weak substrate bonding. However, approximately at the same time, some of the authors of [20] corrected their paper by reporting a significant buckling of the hBN layer of 0.64 Å (total height difference) based on non-contact atomic force microscopy (NC-AFM) and another XSW study [21]. This is a surprising result since the system exhibits only a very weak layer-substrate interaction. While the AFM study seems to reveal a geometric corrugation quite clearly, it is also well known that the (electrostatic) interaction between sample and tip may depend on the electronic structure of the adsorbate system, and hence the observed AFM contrast might still be (partly) due to a modulated electronic structure. We conclude that at this stage it is not completely clear whether the corrugation of hBN/Cu(1 1 1) is of electronic or geometric origin. For the growth study we are presenting in this paper, a possible buckling of the hBN layer will not have any significant impact, and therefore we do not speculate any further on this issue.

In our study we concentrate on the growth behaviour of hBN on Cu(1 1 1) in the submonolayer regime. We present a detailed *in situ* and real-time study based on low-energy electron microscopy (LEEM) and diffraction (LEED). The microscope offers the opportunity to correlate diffraction-based, structural information (obtained from μLEED with sub-μm resolution) with real-time direct space observations of the growth of specific structures using dark-field (DF)-LEEM. We discuss aspects including mobility of step edges, domain formation, domain shape and orientation, and report a dendritic growth pattern exhibiting three-fold symmetry. Finally, based on our findings, we present a growth model that correlates these observations with each other and explains the extraordinary island shape of hBN on Cu(1 1 1).

2. Experimental details

For all experiments, the surface of the Cu(1 1 1) single crystal was cleaned by repeated cycles of sputtering with argon and hydrogen ions (with incident angles of $\pm 15°$ for 15 min each, with $I_{\text{sample}} = 5.4\mu$A and $E_{\text{ion}} = 1$ keV) and subsequent annealing at 950 K for 30 min.

The last annealing step before starting the growth experiment was monitored in LEEM, and higher temperatures (up to 1100 K) were used in order to produce large terraces (about 5–10 μm). For growing hBN, we annealed the crystal at temperatures between 1000 K and 1100 K in borazine ($(HBNH)_3$) atmosphere with a partial pressure of 0.5×10^{-7} to 4.5×10^{-7} Torr. Borazine was purchased from Katchem spol s.r.o, Czech Republic, and continuously stored below 0 °C in order to minimize thermal degradation. The growth of hBN was observed in LEEM in real time. Under the mentioned conditions, a hBN layer is formed on the Cu(1 1 1) surface with an initial growth rate between 0.5 ML h^{-1} and 4.0 ML h^{-1}. As discussed below, the growth of hBN is self-limited and therefore the growth rate is decreasing exponentially with time. We typically observed the growth for several hours. In order to stop the growth the borazine inlet was closed and the sample was cooled down to room temperature with a rate of less than 1 K s^{-1}. Afterwards the cold samples were investigated further.

LEEM measurements were performed using an aberration corrected low-energy electron microscope (Elmitec AC-LEEM 3) having a lateral resolution better than 2 nm. The base pressure of the chamber was below 4×10^{-10} Torr. The microscope allows to obtain electron diffraction patterns from selected areas with diameters smaller than 100 nm (μLEED). In DF-LEEM mode, contrast between different rotational orientations of the same superstructure can be generated. For this purpose an aperture is positioned in a focal plane of the electron optics selecting one diffraction spot for imaging. In this mode only those areas on the surface are imaged bright, which are contributing to this specific diffraction spot. We investigated the growth of the first hBN monolayer (ML) *in situ* and in real-time. All LEEM images were collected using start voltages (U_{start}) below 2 V in bright and below 50 V in dark field mode. No electron beam induced damage of the films could be observed under these imaging conditions.

3. Results and discussion

3.1. Nucleation

We have studied the nucleation of the hBN layer with LEEM in several growth series *in situ* and in real time. Two exemplary images series are shown in figures 1 and 2. A general finding is that no preferred nucleation site could be identified unambiguously, but that islands nucleate on both the clean and flat Cu(1 1 1) surface terraces and at all kinds of defects. The latter includes, in particular, step edges, but also point-like defects like small impurities at the surface. In LEEM such impurities are often visible due to phase contrast, even if their size is below the instrumental resolution. It should be mentioned that step edges, which in

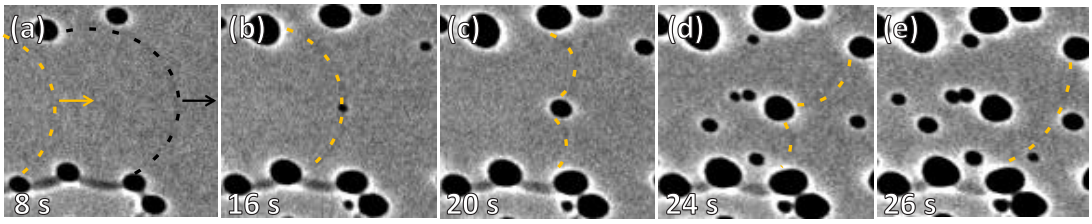

Figure 1. Step edge pinning by a nucleating hBN island: the size of the islands is strongly enhanced because of the chosen imaging conditions ($U_{Start} = 0.8$ V, underfocus). (a) Two copper step edges marked in yellow and black are moving from left to right. (b) An hBN island (dark contrast) nucleates in the middle of the image, just in front of the edge marked in yellow. (c) + (d) This island pins the step edge, which bends around the island. (e) When the step edge encloses the island completely, it is able to pass and move on. The full movie is available as supporting information ('figure-1-moving-step-edges.avi'). (FOV 2.5 μm, 1067 K, 4.5 $\times$ 10^{-7} Torr).

many systems represent preferred nucleation sites, are moving across the surface in our case. The high temperatures (1000–1100 K) that are necessary for growing hBN let Cu atoms desorb from the surface, evidently preferably from the steps, which makes the step edges move across the surface. Figure 1 shows an example. Two step edges are marked with black and yellow dotted lines. Panel (c) shows that the second (yellow) step edge is pinned by an hBN island in the center of the image (dark island nucleating in panel (b) and quickly growing in size in (c)–(e)). Note that in the chosen imaging conditions ($U_{start} = 0.8$ V, underfocus) the step edges can be imaged, but the island size is strongly overestimated (see supporting information section 1.1 for more details (stacks.iop.org/TDM/6/045005/mmedia)). The step edge bends around the island (figures 1(c) and (d)) until the lower terrace is enclosing the entire island; then the step edge is moving on (panel (e)). A similar behavior was observed for step edges passing point defects before the nucleation of hBN started. However, in the example shown in figure 1 there is no point defect present at the location where the yellow edge is pinned. This is proven by the black step edge which is passing the region beforehand without being pinned (see also supporting information, full movie 'figure-1-moving-step-edges.avi').

The observation that the hBN islands are able to pin the moving step edges might be surprising, since the adsorbate-substrate interaction is very weak and the hBN layer is more than 3.2 Å away from the uppermost Cu atoms. However, one should consider that even a slightly delayed desorption of the surface atoms underneath the hBN islands, which we believe can be caused also by a weak interaction, will cause the observe effect of a bending of the step edge. It is not required (and in fact quite unlikely) that the desorption of these atoms is completely inhibited. This is supported by the fact that we cannot observe any indications for buried step edges underneath the hBN islands after these have grown further.

Due to the overestimated island size in underfocus condition the surface appears to be covered completely with hBN long before the layer is actually closing.

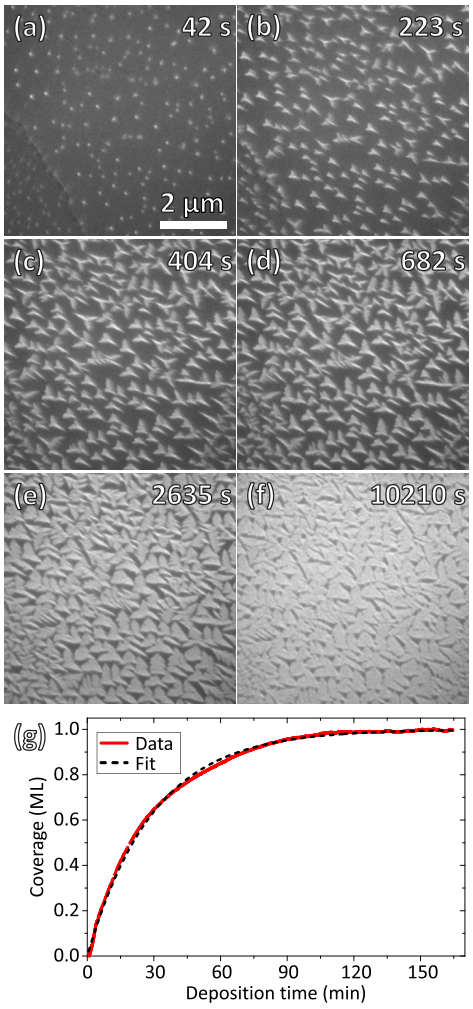

Figure 2. (a)–(f) LEEM images recorded during the growth of hBN on Cu(1 1 1) at 1085 K and a borazine partial pressure of 2.5 $\times$ 10^{-7} Torr ($U_{Start} = 2$ V, slight overfocus). The full movie is available as supporting information ('figure-2-hBN- growth.avi'). (g) hBN coverage for a similar experiment (1015 K, 2.5 $\times$ 10^{-7} Torr), as obtained from the total LEEM intensity, plotted versus deposition time (red line). The data is fitted using a simple exponential relation (black dashed line, see text). The uncertainty in the coverage is estimated to be $<$1%, see supporting information section 1.2. Note that all times given in this work refer to the time after nucleation of the first observable hBN islands. Time scales for the image series (a)–(f) and the coverage plot (g) differ due to different growth rates (caused by different substrate temperatures).

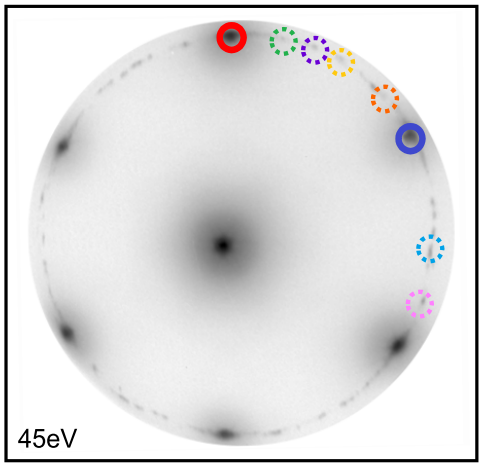

Figure 3. μLEED pattern of an almost closed monolayer hBN on Cu(1 1 1) at $U_{Start} = 45$ V. A modulated ring of LEED intensity is visible, stemming from differently rotated hBN domains, and relatively sharp spots close to the Cu(1 1 1) spots from aligned domains with a strongly preferred azimuthal orientation. The spots used for the DF-LEEM images in figures 4 and 5 are marked by solid and dashed circles, respectively.

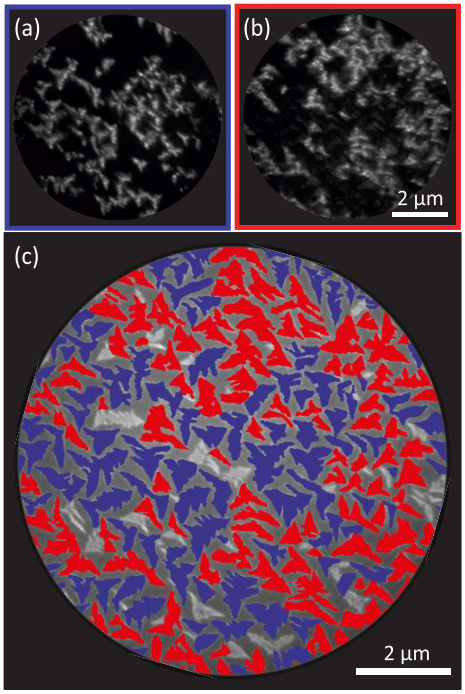

Figure 4. ((a),(b)) DF-LEEM images of the two types of aligned domains of hBN on Cu(1 1 1), grown at 1025 K and 1.0×10^{-7} Torr ($U_{Start} = 45$ V). LEED spots used for the DF-LEEM images shown in (a) and (b) are marked with blue and red circles in figure 3, respectively. (c) LEEM image of the same field of view ($U_{start} = 2$ V). Aligned islands, as identified by the DF-LEEM measurements shown in (a) and (b), are colored in blue and red, respectively.

Therefore, the movement of step edges cannot be observed any more at higher hBN coverages (for more details, see supporting information section 1.1). But we assume that the movement of step edges continues until most of the surface is covered, i.e. until a very high density of pinning centers is present, just as it is the case for metal crystals with a high density of defects. In conclusion, we find that nucleating hBN islands influence the movement of step edges across the surface, but reversely, the moving step edges have no significant influence on the growth of the hBN islands.

3.2. Growth rate

In figure 2, a series of LEEM images shows the growth of hBN on Cu(1 1 1) at 1085 K and a borazine pressure of 2.6×10^{-7} Torr. In contrast to figure 1, the imaging conditions are changed to slight overfocus and $U_{start} = 2$ V. This inverses the contrast so that hBN islands appear bright on the dark Cu(1 1 1) surface, their apparent size and shape are now close to reality. Step edges are no longer visible under these imaging conditions. From the time of nucleation, the islands appear to be dendritic and show triangular contour lines. From the image series in figure 2, which is recorded at constant substrate temperature and partial borazine pressure, it can clearly by seen that the growth rate is significantly decreasing with deposition time and increasing coverage. Under these imaging conditions, the total coverage can be well quantified by measuring the integrated intensity of the entire LEEM images. This is even true for small changes in the focus settings, as shown in more detail in the supporting information section 1.2. In figure 2(g) we plot the total coverage, as obtained from the integrated LEEM intensity, versus the deposition time for a growth experiment performed at very similar conditions (1015 K and 2.5×10^{-7} Torr). The resulting curve is shown as a red line and can be fitted using

$$A(t) = 1 - e^{-\frac{t}{\lambda}}, \quad (1)$$

which indicates that the growth rate $\frac{d}{dt}A$ is proportional to the uncovered surface area $(1 - A)$ (A represents the hBN covered surface area) [11, 22–24]. Therefore, we can clearly conclude that the clean and hot Cu surface is necessary for the reaction of borazine to hBN to take place, leading to a self-limitation of the growth of hBN on Cu(1 1 1). A similar behavior was found for hBN on Ni(1 1 1) [17], Ag(0 0 1) [22], Cu(1 1 0) [24], Pt(1 1 1) [25], Ir(1 1 1) [23, 26] and Ru(0 0 0 1) [11], see also [13].

3.3. Domain structure

For investigating the structure of the individual domains of hBN on Cu(1 1 1) we applied μLEED and DF-LEEM. Figure 3 depicts a μLEED image of an hBN layer on Cu(1 1 1) close to one monolayer coverage. A modulated ring of diffraction intensity and six relatively broad spots are clearly visible, the latter lying almost on top of the Cu bulk reflections. When LEED is performed with higher k-space resolution (see SPA-LEED image shown as figure 1 in Brülke *et al* [15]), it can be seen that both ring and hBN-spots are not precisely matching with the Cu bulk LEED spots (see also supporting information section 2.1). The six hBN

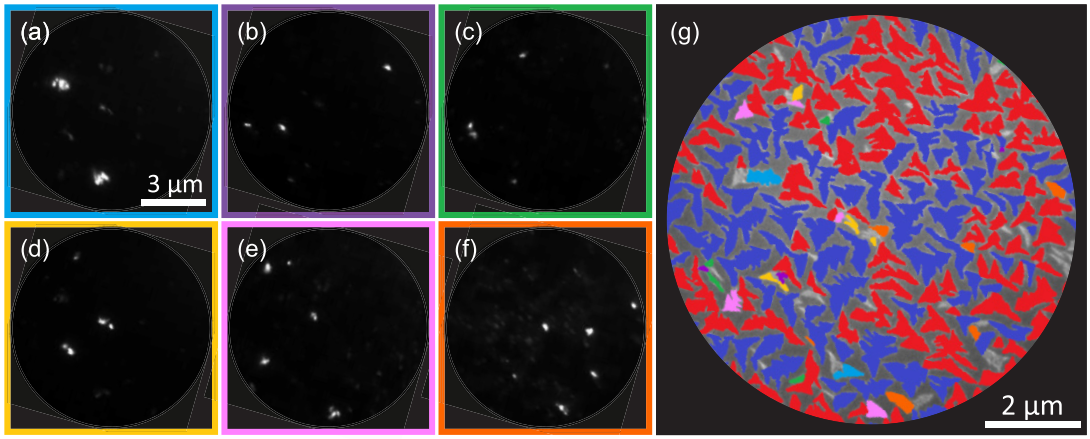

Figure 5. ((a)–(f)) DF-LEEM images of rotated hBN domains on Cu(1 1 1) (same growth conditions as in figure 4). Six different aperture positions along the diffraction ring were selected, as indicated in figure 3 by dashed circles in the corresponding colors. (g) False color illustration of all domains discussed so far. The remaining (gray) domains correspond to other aperture positions along the diffraction ring, i.e. to other domain orientations. (FOV 10 μm).

reflections are much more intense than the modulated ring, indicating that the majority of domains are well aligned with the substrate ('aligned domains'). For the minority domains the modulated diffraction ring proofs various azimuthal orientations ('rotated domains').

DF-LEEM allows us to investigate the distribution of islands with various azimuthal orientations in more detail. By inserting an aperture in the beam path, a certain LEED spot is selected for imaging and only those parts of the surface appear bright that contribute to this LEED spot. We have performed this for the blue and red marked spots in figure 3, corresponding to the (10) and (01) reflections of the hBN structure. Due to the three-fold symmetry of the hBN structure, these reflections are inequivalent in electron diffraction, and therefore they have different intensities (for details see supporting information section 3). However, the six-fold symmetry of the uppermost substrate atomic layer also allows the formation of a second type of aligned hBN islands, which is rotated by 60° with respect to the first. For this domain type the positions of the (10) and (01) reflections are swapped, so that we find superimposed intensities of the (10) spot of the first and the (01) spot of the second type of aligned domains at the blue marked spot in figure 3, and vice versa for the red spot. In other words, in the experiment both spots contain some intensity from both aligned domains, but with a different ratio, and therefore these spots can be used to identify the two different types of aligned domains in DF-LEEM, as discussed in the following.

In figures 4(a) and (b) DF-LEEM images using the (10) and (01) spot (blue and red circles in figure 3), respectively, are depicted. Panel c shows a false-color image with the two DF-LEEM images a and b colored red and blue, respectively, and being superimposed on a BF-LEEM image with the same field of view. In this image about 95% of the islands belong to one of these aligned domains, indicating that this is the strongly preferred orientation of islands. For more details on the (very narrow) azimuthal distribution of the aligned domains see supporting information section 2.2. Additionally, there are the rotated domains, which are visible as gray (uncolored) areas in figure 4(c) and show a slightly different contrast in BF-LEEM compared to the aligned domains (see supporting information section 2.3). The latter might indicate a different interaction with the substrate. These rotated islands can also be identified in DF-LEEM for aperture positions along the diffraction ring. In figure 5 we show this for six exemplary positions. The individual DF-LEEM images are shown in panels (a)–(f), the corresponding false color image is depicted in (g). The corresponding aperture positions are indicated in figure 3 (dotted rings in the same color code). All other domains (i.e. those not colored in figure 5(g)) correspond to other positions on the diffraction ring.

Overall, our findings are in very good agreement with the results obtained by Schwarz *et al* [21] and Brülke *et al* [15]. A much stronger modulation of the diffraction ring seen in our experiments compared to the LEED and SPA-LEED images shown in figure 1(b) of [21] and figure 1(a) of [15] can be explained by the illuminated surface area which is below 20 μm^2 in our case, whereas it is in the mm^2-range for the LEED images presented in the two mentioned papers. Therefore, our μLEED image shows a much smaller selection of rotated domains compared to the (SPA-)LEED images presented by Brülke *et al* and Schwarz *et al*. In conclusion, we state that the diffraction ring is formed by several islands with various azimuthal orientations (continuously, but not equally distributed) that can be well localized in DF-LEEM. The clear majority of domains, however, is well aligned with the substrate. They fall into two groups, with their lattices oriented 0° and 60° with respect to the substrate lattice.

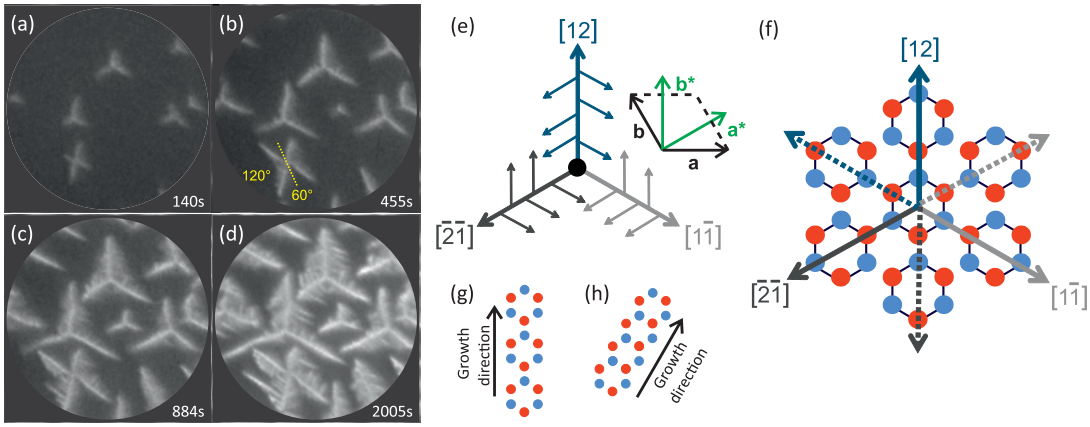

Figure 6. (a)–(d) BF-LEEM images showing the dendritic growth of hBN islands (FOV 3.5 μm, start voltage 2 V, slight overfocus, temperature 1035 K, partial borazine pressure 0.5×10^{-7} Torr): main branches grow in three preferred growth directions with an angle of 120° relative to each other. When they approach neighboring islands, side branches start to grow diverting backwards from the main branches, again under an angle of 120°. In the lower left a twinned island with four growth branches is visible. A yellow dotted line in (b) indicates the domain boundary separating the two structures, and yellow numbers indicate the angles between the four growth branches. For more details see text. The full movie is available as supporting information ('figure-6-dendritic-growth.avi'). (e) Schematic representation of the dendritic growth. The three preferred growth directions are given in real space coordinates, corresponding to $(0\ 1)$, $(\bar{1}\ 0)$ and $(1\ \bar{1})$ directions in reciprocal space. (f) Growth via three of the hexagon corners (solid arrows) is preferred over the other three hexagon corners (dotted lines) and the hexagon sides. (g) Illustration of the growth of hBN in the directions of the corners of the hexagon and (h) via its sides.

3.4. Preferred growth directions

We now turn to a discussion of the growth of individual hBN islands. Figures 6(a)–(d) show enlarged LEEM images recorded during growth. It can clearly be seen that the islands grow in three preferred directions having an angle of 120° with respect to each other. The main branches grow quickly in length (see panels (a)–(c)), until they approach the branches of the neighboring islands. Side branches start to grow as well, diverting backwards from the main branches, again under an angle of 120°, see panels (c)–(d). The growth of these side branches seems to be hindered as long as the main branches still have enough space to grow forward. The slight increase in brightness of the main branches observed with time, indicating a slight broadening of the branches, can be explained by the beginning growth of the side branches, see also below. A schematic illustration of this growth mode is depicted in figure 6(e). Note that one apparent exception to the observation of three growth branches can be found in the LEEM images (figures 6(a)–(d)): an island in the lower left exhibits four main growth branches. This island is a twin consisting of two domains. The boundary between the two domains is indicated by the dotted yellow line in panel (b) and runs right through the nucleation point of the island. The two growth branches visible on each side of the boundary belong to the same domain, and therefore include an angle of 120° with each other. To the neighboring branch of the other domain they form a 60° angle, caused by the 60° rotation angle between the lattices of the two domains.

Since the LEEM instrument enables us to directly correlate growth directions (in real space) with the orientation of LEED patterns (directions in reciprocal space), we are able to unambiguously identify the crystallographic growth direction of these hBN branches. (See supporting information section 4 for the non-trivial procedure of correlating direct and reciprocal space directions in LEEM.) As a result, we identify the three preferred growth directions as $[1\ 2]$, $[\bar{2}\ \bar{1}]$ and $[1\ \bar{1}]$ in real space (corresponding to $(0\ 1)$, $(\bar{1}\ 0)$ and $(1\ \bar{1})$ in reciprocal space), as illustrated in figures 6(e) and (f). This demonstrates that the growth via three of the six corners of the hBN hexagon is preferred over all other directions (solid arrows in figure 6(f), see also panel (g)), in particular over the other three hexagon corners (dotted lines), and over the sides of the hexagon (figure 6(h)). Comparing figures 6(g) and (h) shows that growth via the corners does not require the destruction of the B_3N_3 hexagon during the growth process but allows to attach the intact borazine molecule (after some dehydrogenation), in contrast to a growth via the hexagon sides.

3.5. Growth model

The growth of fractal (and also dendritic) islands is often discussed in the framework of diffusion-limited aggregation (DLA), see e.g. [27] and references therein. This growth model was originally suggested by Witten and Sander in 1981 based on computer simulations [28]. It describes the growth in terms of diffusion of free atoms on the surface, and their adhesion to an existing island when they enter a certain 'capture zone' around the island ('hit-and-stick'). Such structures are usually fractal, not dendritic, i.e. the growth branches are randomly oriented and do not show any preferred growth direction or orientation [28]. However, in our case of hBN/Cu(11) we have to deal with molecular adsorbates and, as discussed above, we clearly find strongly preferred growth directions rather than

randomly oriented branches. Therefore, other effects must be influencing the growth, which are responsible for the three-fold symmetry observed in our study.

Our most remarkable observation is that only three (not six) main growth branches occur, forming three-fold symmetric islands of the growing hBN fractals. This is unexpected since all six possible directions (those across the corners of the B_3N_3 hexagon) appear to be equivalent, as illustrated in figure 6(f). We found that this is valid for all types of domains, in particular for the two aligned domain types, but also for the rotated domains. One seemingly obvious reason for this observation might be the substrate, simply because the Cu(1 1 1) surface is also three-fold symmetric, only the structure of the uppermost Cu layer has six-fold symmetry. Consequently, as soon as the second bulk layer plays a role in the interaction between hBN islands and the substrate, one might expect a three-fold instead of a six-fold symmetric pattern for the hBN domains. However, in such a case, it would be unexpected to observe *two* aligned domains, since the atomic arrangement for the main branches of the second, 60° rotated domain would be identical to that of the suppressed branches of the first domain. This suggests that the reason for the three preferred growth directions lies in an interaction mechanism within the hBN layer, not in the symmetry of the substrate.

The experimental finding that growth along the dashed and solid arrows in figure 6(f) are not equivalent, can be broken down to an asymmetry in the adhesion energy for the different ways a borazine molecule can approach an existing hBN island, namely either with one of its nitrogen atoms to a boron atom of the island, or vice versa, with a boron atom of the molecule to a nitrogen atom of the island. This is illustrated in figure 7(a): the blue-filled molecule labeled 'i' (island) represents the last one of a branch of the already existing hBN island, growing towards the lower left. Molecule '1' attaches with its 'red' atom to a 'blue' one of the existing island, while molecule '2' bonds with a 'blue' atom to a 'red' one of the island. The conclusion from our experimental findings is that the first scenario is preferred while the second is strongly suppressed, i.e. the branch continues growing straight to the lower left rather than bending by 60°. The third scenario illustrated in figure 7(a), namely that one molecule attaches to the sides of the existing main branch, seems to be suppressed as well, at least as long as the main branches still have space to grow further. In this early growth stage the forward growth of the branches is much faster than the increase of their thickness or any sideward growth. However, occasionally some short side branches are visible already (see e.g. figures 6(b) and (c)), and hence scenario scenario '3' is not strictly inhibited. As soon as the forward growth comes to an end due to the proximity of the neighboring islands, the side branches start to grow much faster.

Note that the first molecule of the side branch forms two bonds to the original hBN chain, one blue-red and one red-blue (scenario '3' in figure 7(a)). But for the second and all following molecules of the side branch the situation is identical to the growth of the main branch: a red atom of the molecule forms the bond to a blue one of the island (scenario '1' in figure 7(a)), and thus defines the forward direction for the side branch. This results in the observed angle of 120° between the growth directions of the main branch in its side branches, as illustrated in figure 7(b). Scenario '2', and therefore the 60° growth direction, is again suppressed. With progressing growth the ramification of the branches continues, until in the end the molecules are also forced into unfavored adhesion sites simply due to the incremental filling of the available space.

We would like to mention, that this growth model can also explain the observation of the second type of aligned domains which are rotated by 60° (see figure 4 and discussion above). As long as the interaction of both atomic species with the substrate does not differ too much, islands with inverted structure (i.e. with boron and nitrogen interchanged, which is equivalent to a 60° rotation of the structure) should also be stable and show the same growth behavior. Interchanging B and N also swaps the preferred and suppressed growth directions for both main and side branches, and hence explains why the second aligned domains look like mirror domains of the first.

The remaining question is the one for the origin of the asymmetry in the adhesion energies for the formation of N_{mol}-B_{isl} and B_{mol}-N_{isl} bonds. (The indices 'mol' and 'isl' indicate whether the atom is part of the attaching molecule or the existing island, respectively.) On a semi-quantitative basis, one may argue from bonding energies for the free borazine molecule that have been calculated by Auwärter *et al* [29]. Although the absolute values of the reported energies appear to be very (maybe unrealistically) high, they very clearly indicate that the B-H bond is weaker than that of N-H, in the gas phase by more than 0.5 eV in bonding energy. We can therefore conclude that the energies for dehydrogenation of both N and B also differ significantly after the molecule has adsorbed on the rather reactive Cu(1 1 1) surface, and the same is certainly true for the terminating atoms of the hBN islands. This in turn may cause different dehydrogenation states for the hBN islands and the borazine molecules adsorbed on the surface. Consequently, the adhesion energy for a borazine molecule attaching to an island via an N_{mol}-B_{isl} bond will differ from the energy involved in the B_{mol}-N_{isl} bond formation, which is exactly what we concluded from our experimental results. Two possibilities for such a scenario are sketched in figures 7(c) and (d): if we assume that the hBN islands are completely dehydrogenated, while the attaching molecule is not—this scenario is illustrated in panel (c)—one

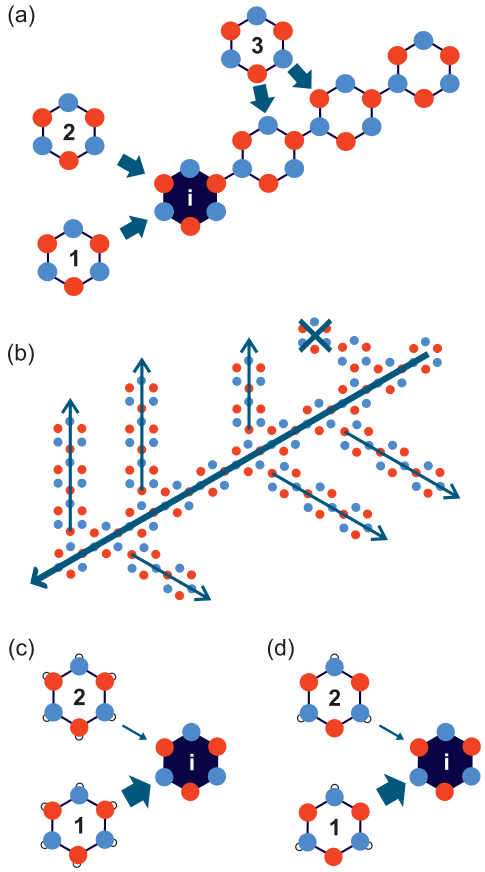

Figure 7. (a) Illustration of the three ways a borazine molecule can attach an existing hBN island: the B_3N_3 ring labeled 'i' represents the last ring of the existing island. Molecule '1' attaches with one of its 'red' atoms to a 'blue' atom of the existing hBN island, and vice versa ('blue' to 'red') for molecule '2'. Molecule '3' forms two such bonds, one of each kind. As an experimental fact, scenario '1' is strongly preferred over the others as long as only the main branches are growing. (b) Illustration of the growth directions of the side branches: occasionally, a molecule attaches to the side of the main branch (according to scenario '3'). After this has happened, scenario '1' is again preferred, leading to side branches that are back-folded by 120° with respect to the main branch. (c) and (d) Illustration of possible reasons for unequal adhesion energies for the two adhesion scenarios: a hydrogenated (c) and partially dehydrogenated (d) borazine molecule attaches to a fully dehydrogenated hBN island. Note that we cannot assign red and blue to the two atomic species.

has to remove one H atom from the borazine molecule, either from a nitrogen atom or from a boron atom, in order to attach the molecule to the island. If we further assume that the significant difference between the B-H and N-H bonding energies found for the gas phase is at least partly preserved for molecules adsorbed on the Cu(1 1 1) surface, the formation of a bond between the molecule-boron and the hBN-nitrogen atom (B_{mol}-N_{isl}) would be favored over the alternative scenario, a N_{mol}-B_{isl} bond. The same result is obtained if the attaching borazine molecule is already partially dehydrogenated, see figure 7(d): in this case, the B_{mol}-N_{isl} could attach without any further dehydrogenation process, whereas for N_{mol}-B_{isl} bonding the N-H bond still has to be broken. Other scenarios with similar results are possible, e.g. with partly dehydrogenated hBN islands. However, the decisive feature of all scenarios that can explain our observation is a difference in the dehydrogenation state of hBN islands and the borazine molecule before it attaches the island.

Although these qualitative considerations are somewhat speculative, they demonstrate that there are simple (energetic) mechanisms that favor the asymmetry in adhesion energies we have deduced from our experimental data. The growth model we suggest is therefore not only realistic, but also generic for molecular adsorbate systems that exhibit the mentioned asymmetry of adhesion energies for the relevant growth channels. We entitle this growth mechanism 'Dehydrogenation Limited Aggregation', since the different dehydrogenation states of the aggregating objects represent the key condition for this particular growth behavior, which in our specific case is characterized by dendritic hBN islands.

Finally, we discuss the growth of hBN/Cu(1 1 1) in context with studies of hBN on other substrates. Most of them were performed on more reactive surfaces like, e.g. Ni(1 1 1), Ru(0 0 0 1), Rh(1 1 1), and Ir(1 1 1). On these substrates compact, triangular islands have been reported [26, 29–33], and the observation of atomic boron [23, 34, 35] or boron islands at low temperatures [26] indicates that borazine does not only dehydrogenate, but that the B_3N_3 ring decomposes upon adsorption on these surfaces. Consequently, not (only) intact molecules, but also fragments attach to existing islands and form compact islands that are terminated by one species, causing the triangular shape. It is an ongoing discussion whether nitrogen [29–31] or boron [36] is the terminating species.

Our growth model for the case of hBN/Cu(1 1 1) does not require that the B_3N_3 ring decomposes, the model rather assumes that intact (at best dehydrogenated) molecules attach to the existing islands on the surface, and the triangular shape is a consequence of three preferred growth directions. This is consistent with the fact that no indications for atomic boron was found for hBN on Cu(1 1 1)—neither in our studies, nor by Brülke *et al* [15, 37] who applied the same preparation scheme—or for hBN on Ag(1 1 1) [14] and Ag(0 0 1) [22]. Apparently, the surfaces of these noble metals are not reactive enough to crack the B_3N_3 ring, in contrast to the transition metal surfaces mentioned above. The different reactivities of these surfaces are also reflected by growth rates and dosages which have been used. While on the transition metal surfaces dosages below 100 L were sufficient for growing a monolayer of hBN, these numbers are higher by at least a factor of 20 for the nobel metal surfaces (for details see supporting information section 5).

4. Summary

We have investigated the growth of hBN on Cu(1 1 1) *in situ* and in real time using LEEM and μLEED.

Beside studying the movement of step edges across the surface and their interaction with impurities and nucleating hBN islands, we concentrated on the growth of hBN islands from nucleation to closing of the first layer. The growth is self-limited to one single layer since the reactive Cu(1 1 1) surface is obviously essential for the formation of the hBN layer. As soon as the Cu surface is covered, the growth comes to a halt.

In contrast to what one might expect from earlier studies on many other substrates, we found no compact islands on the surface, but we observed dendritic growth of the structures, clearly exhibiting three different preferred growth branches within each island. The orientation of the islands, in turn, is varying. By far the majority of islands belongs to two aligned domains that are oriented either 0° or 60° to the underlying substrate lattice. The remaining islands exhibit a continuous but not random distribution of their azimuthal orientation.

We explain the dendritic growth by a model based on our experimental findings and some considerations of adhesion and dehydrogenation energies. From LEEM and LEED experiments we were able to correlate the preferred growth directions with the crystallographic [12]-direction (and its symmetry equivalents), which corresponds to three of the six corners of the B_3N_3 hexagon (as illustrated in figure 6). It is highly interesting that the growth takes place only in the direction of three of the six corners, those which are occupied by the same atomic species. We explain this by an asymmetry in the adhesion energy for the two relevant processes: apparently, it is favorable to attach a borazine molecule with its atomic species 'A' to an atom of species 'B' of the existing hBN island. The alternative process, attaching the molecule with species 'B' to an 'A' atom of hBN, is suppressed. This asymmetry of adhesion energies can conclusively explain all our experimental findings. Based on bond energies from the literature we speculate that 'A' is boron, and 'B' is nitrogen, i.e. that the molecules attach with a boron atom to a nitrogen atom of the island.

Furthermore, we suggest that the asymmetry of adhesion energies is caused by different dehydrogenation states for the borazine molecule adsorbed on the surface and the hBN island. Since the growth behavior of the hBN islands is therefore determined by dehydrogenation of the aggregating objects, we call this mechanism 'Dehydrogenation Limited Aggregation'. The different dehydrogenation states, in turn, are probably due to an accidental (and fortunate) moderate strength of the interaction between the borazine (and hBN) and the substrate. Compared to other metal substrates, hBN and borazine exhibit an intermediate interaction with Cu(1 1 1): it is (much) weaker than for transition metals, but stronger than for Ag(0 0 1) and (1 1 1). We therefore suggest that the dendritic growth of hBN/Cu(1 1 1) is caused by different dehydrogenation states of borazine and hBN on Cu(1 1 1), which in turn is a consequence of the intermediate interaction strength between adsorbate and substrate.

Acknowledgments

Financial support from the Helmholtz-Gemeinschaft deutscher Foschungszentren (HGF) and the Deutsche Forschungsgemeinschaft via the Collaborative Research Center SFB 1083 is gratefully acknowledged.

ORCID iDs

Christian Kumpf https://orcid.org/0000-0003-3567-5377

References

[1] Watanabe K, Taniguchi T and Kanda H 2004 *Nat. Mater.* **3** 404–9
[2] Xu M, Liang T, Shi M and Chen H 2013 *Chem. Rev.* **113** 3766–98
[3] Geim A K and Grigorieva I V 2013 *Nature* **499** 419–25
[4] Dean C R *et al* 2010 *Nat. Nanotechnol.* **5** 722–6
[5] Kim K K *et al* 2011 *Nano Lett.* **12** 161–6
[6] Siegel G, Ciobanu C V, Narayanan B, Snure M and Badescu S C 2017 *Nano Lett.* **17** 2404–13
[7] Laskowski R, Blaha P, Gallauner T and Schwarz K 2007 *Phys. Rev. Lett.* **98** 106802
[8] Preobrajenski A B, Nesterov M A, Ng M L, Vinogradov A S and Mårtensson N 2007 *Chem. Phys. Lett.* **446** 119–23
[9] Song L *et al* 2010 *Nano Lett.* **10** 3209–15
[10] Corso M, Auwärter W, Muntwiler M, Tamai A, Greber T and Osterwalder J 2004 *Science* **303** 217–20
[11] Sutter P, Lahiri J, Albrecht P and Sutter E 2011 *ACS Nano* **5** 7303–9
[12] Hibino H, Wang S, Orofeo C and Kageshima H 2016 *Prog. Cryst. Growth Ch.* **62** 155–76
[13] Auwärter W 2019 *Surf. Sci. Rep.* **74** 1–95
[14] Müller F, Hüfner S, Sachdev H, Laskowski R, Blaha P and Schwarz K 2010 *Phys. Rev.* B **82** 113406
[15] Brülke C, Heepenstrick T, Humberg N, Krieger I, Sokolowski M, Weiß S, Tautz F S and Soubatch S 2017 *J. Phys. Chem.* C **121** 23964–73
[16] Schulz F, Drost R, Hämäläinen S K, Demonchaux T, Seitsonen A P and Liljeroth P 2014 *Phys. Rev.* B **89** 235429
[17] Auwärter W, Kreutz T J, Greber T and Osterwalder J 1999 *Surf. Sci.* **429** 229–36
[18] Preobrajenski A B, Vinogradov A S, Ng M L, Ćavar E, Westerström R, Mikkelsen A, Lundgren E and Mårtensson N 2007 *Phys. Rev.* B **75** 245412
[19] Schulz F, Drost R, Hämäläinen S K and Liljeroth P 2013 *ACS Nano* **7** 11121–8
[20] Joshi S *et al* 2012 *Nano Lett.* **12** 5821–8
[21] Schwarz M *et al* 2017 *ACS Nano* **11** 9151–61
[22] Müller F and Grandthyll S 2013 *Surf. Sci.* **617** 207–10
[23] Orlando F, Larciprete R, Lacovig P, Boscarato I, Baraldi A and Lizzit S 2012 *J. Phys. Chem.* C **116** 157–64
[24] Herrmann C, Omelchenko P and Kavanagh K L 2018 *Surf. Sci.* **669** 133–9
[25] Zhang Y, Weng X, Li H, Li H, Wei M, Xiao J, Liu Z, Chen M, Fu Q and Bao X 2015 *Nano Lett.* **15** 3616–23
[26] Petrović M, Hagemann U, Horn-von Hoegen M and Meyer zu Heringdorf F J 2017 *Appl. Surf. Sci.* **420** 504–10
[27] Michely T and Krug J 2004 *Islands, Mounds and Atoms* (Berlin: Springer)
[28] Witten T A Jr and Sander L M 1981 *Phys. Rev. Lett.* **47** 1400–3
[29] Auwärter W, Suter H, Sachdev H and Greber T 2004 *Chem. Mater.* **16** 343–5
[30] Auwärter W, Muntwiler M, Osterwalder J and Greber T 2003 *Surf. Sci.* **545** L735–40

[31] Lu J, Yeo P S E, Zheng Y, Xu H, Gan C K, Sullivan M B, Castro Neto A H and Loh K P 2013 *J. Am. Chem. Soc.* **135** 2368–73
[32] Dong G, Fourré E B, Tabak F C and Frenken J W 2010 *Phys. Rev. Lett.* **104** 096102
[33] Poelsema B, Acun A, Schouten L, Derkink F, Tsvetanova M, Zhang Z, Zandvliet H J W and van Houselt A 2019 *2D Mater.* **6** 035010
[34] Kidambi P R, Blume R, Kling J, Wagner J B, Baehtz C, Weatherup R S, Schloegl R, Bayer B C and Hofmann S 2014 *Chem. Mater.* **26** 6380–92
[35] Preobrajenski A B, Vinogradov A S and Mårtensson N 2005 *Surf. Sci.* **582** 21–30
[36] Farwick zum Hagen F H *et al* 2016 *ACS Nano* **10** 11012–26
[37] Brülke C 2017 private communications